WIDG Journal Club

Cosmic Axion Spin Precession Experiment

B. Brubaker A. Malagon

Yale University

11/18/2013

Overview

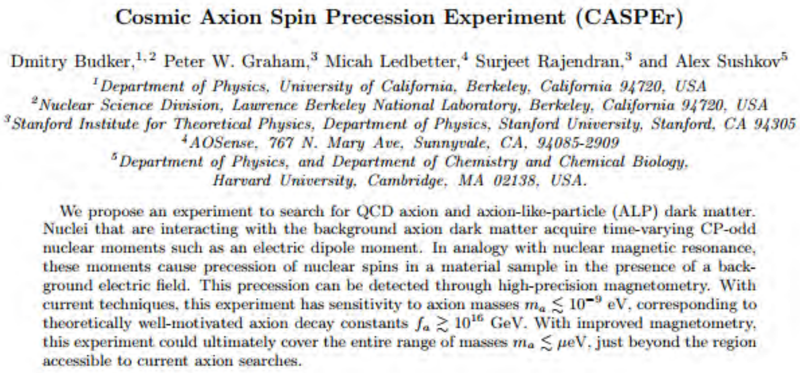

Cosmic Axion Spin Precession Experiment (CASPEr)

Dmitry Budker,[1,2] Peter W. Graham,[3] Micah Ledbetter,[4] Surjeet Rajendran,[3] and Alex Sushkov[5]
[1] *Department of Physics, University of California, Berkeley, California 94720, USA*
[2] *Nuclear Science Division, Lawrence Berkeley National Laboratory, Berkeley, California 94720, USA*
[3] *Stanford Institute for Theoretical Physics, Department of Physics, Stanford University, Stanford, CA 94305*
[4] *AOSense, 767 N. Mary Ave, Sunnyvale, CA, 94085-2909*
[5] *Department of Physics, and Department of Chemistry and Chemical Biology, Harvard University, Cambridge, MA 02138, USA.*

We propose an experiment to search for QCD axion and axion-like-particle (ALP) dark matter. Nuclei that are interacting with the background axion dark matter acquire time-varying CP-odd nuclear moments such as an electric dipole moment. In analogy with nuclear magnetic resonance, these moments cause precession of nuclear spins in a material sample in the presence of a background electric field. This precession can be detected through high-precision magnetometry. With current techniques, this experiment has sensitivity to axion masses $m_a \lesssim 10^{-9}$ eV, corresponding to theoretically well-motivated axion decay constants $f_a \gtrsim 10^{16}$ GeV. With improved magnetometry, this experiment could ultimately cover the entire range of masses $m_a \lesssim \mu$eV, just beyond the region accessible to current axion searches.

Overview

- Axions: hypothetical particles that might

Overview

- Axions: hypothetical particles that might
    - Solve the strong CP problem

Overview

- Axions: hypothetical particles that might
  - Solve the strong CP problem
  - Constitute all or part of the dark matter

Overview

- Axions: hypothetical particles that might
  - Solve the strong CP problem
  - Constitute all or part of the dark matter
- Overview of parameter space and current detection strategies: often unfavorable scaling with small coupling constants

Overview

- Axions: hypothetical particles that might
  - Solve the strong CP problem
  - Constitute all or part of the dark matter
- Overview of parameter space and current detection strategies: often unfavorable scaling with small coupling constants
- One measurable effect: dark matter axion field induces oscillating EDMs in nucleons

Overview

- Axions: hypothetical particles that might
  - Solve the strong CP problem
  - Constitute all or part of the dark matter
- Overview of parameter space and current detection strategies: often unfavorable scaling with small coupling constants
- One measurable effect: dark matter axion field induces oscillating EDMs in nucleons
- CASPEr plans to search for this effect using NMR techniques.

The Strong CP Problem

The Strong CP Problem

- *CP* Violation (equivalent to *T* Violation by CPT Theorem): A question of fundamental importance in particle physics and cosmology

The Strong CP Problem

- *CP* Violation (equivalent to *T* Violation by CPT Theorem): A question of fundamental importance in particle physics and cosmology
- *T*-symmetry violation parametrized by a phase: e.g., $V \rightarrow Ve^{i\theta}$ in Schroedinger equation.

The Strong CP Problem

- *CP* Violation (equivalent to *T* Violation by CPT Theorem): A question of fundamental importance in particle physics and cosmology
- *T*-symmetry violation parametrized by a phase: e.g., $V \rightarrow Ve^{i\theta}$ in Schroedinger equation.
- QCD Lagrangian contains *CP*-violating term $\mathcal{L}_\theta \propto \theta G\widetilde{G}$
- $\theta =$ sum of free parameters from strong and electroweak sectors: theory suggests $\theta \sim \mathcal{O}(1)$, but experiments constrain $\theta < 10^{-10}$ $\Rightarrow$ *The Strong CP Problem*

Symmetry Violation and EDMs

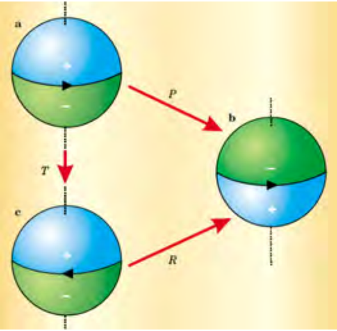

Symmetry Violation and EDMs

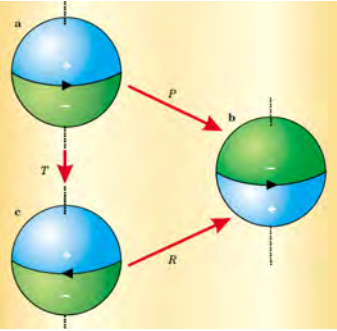

- By Wigner-Eckart Theorem, expectation values of vector operators must point along spin quantization direction

Symmetry Violation and EDMs

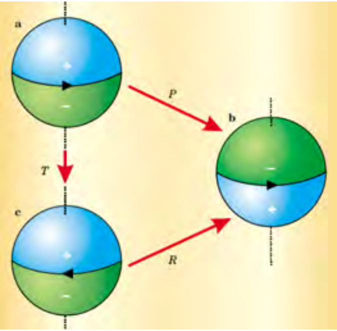

- By Wigner-Eckart Theorem, expectation values of vector operators must point along spin quantization direction
- Magnetic and Electric Dipole Moments transform oppositely under P and T reversal

Symmetry Violation and EDMs

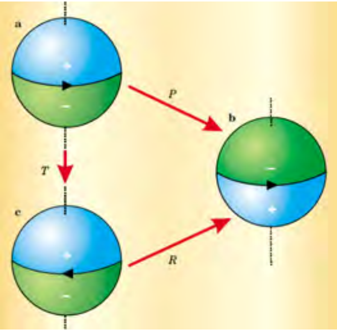

- By Wigner-Eckart Theorem, expectation values of vector operators must point along spin quantization direction
- Magnetic and Electric Dipole Moments transform oppositely under *P* and *T* reversal
- *CP* violation in QCD $\Rightarrow$ neutron EDM. Non-observation constrains $\theta < 10^{-10}$ rad

Solving the Strong *CP* Problem: Axions

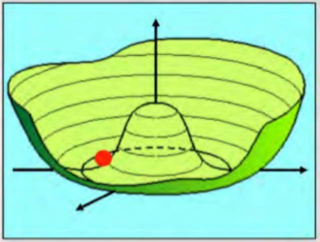

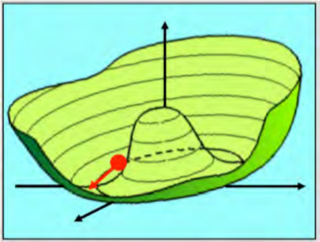

Solving the Strong *CP* Problem: Axions

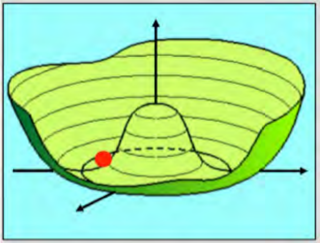

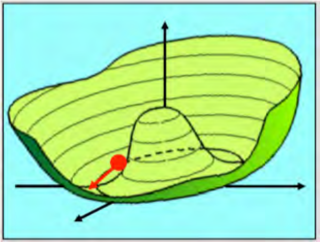

- Introduce complex pseudoscalar field A with $U(1)$ symmetry in $a = \arg[A]$: coupling to QCD yields $\theta = \frac{a}{f_a}$

Solving the Strong *CP* Problem: Axions

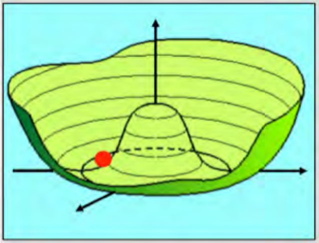

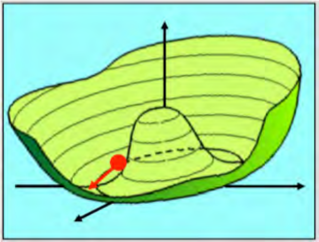

- Introduce complex pseudoscalar field A with $U(1)$ symmetry in $a = \arg[A]$: coupling to QCD yields $\theta = \frac{a}{f_a}$
- Spontaneous symmetry breaking at energy scale f_a produces "Mexican hat" potential

Solving the Strong *CP* Problem: Axions

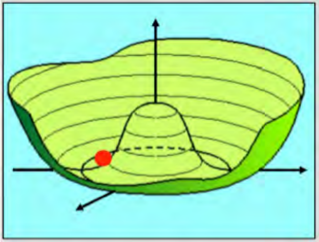

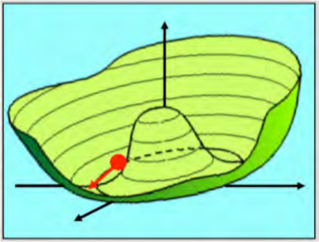

- Introduce complex pseudoscalar field A with $U(1)$ symmetry in $a = \arg[A]$: coupling to QCD yields $\theta = \frac{a}{f_a}$
- Spontaneous symmetry breaking at energy scale f_a produces "Mexican hat" potential
- QCD instanton effects tilt potential: $\theta \to 0$ dynamically. Zero-point fluctuations w/ mass $m_a \sim \Lambda^2_{\mathrm{QCD}}/f_a \Leftrightarrow$ *axions*

Axion Dark Matter

$$\mathcal{L} = \frac{1}{2}(\partial^\mu a)^2 - \frac{1}{2}m_a^2 a^2 + C\frac{a}{f_a}G\widetilde{G} + C'\frac{a}{f_a}F\widetilde{F} + \cdots$$

- Couplings scale as $g \propto f_a^{-1} \propto m_a$
- $\Rightarrow$ Low-mass axions ($m_a < 1$ meV) could be dark matter!

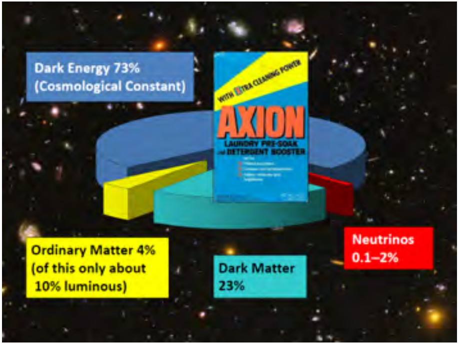

Properties of Axion Dark Matter

$$\mathcal{L} = \frac{1}{2}(\partial^\mu a)^2 - \frac{1}{2}m_a^2 a^2 + C\frac{a}{f_a}G\widetilde{G} + C'\frac{a}{f_a}F\widetilde{F} + \cdots$$

Properties of Axion Dark Matter

$$\mathcal{L} = \frac{1}{2}(\partial^\mu a)^2 - \frac{1}{2}m_a^2 a^2 + C\frac{a}{f_a}G\widetilde{G} + C'\frac{a}{f_a}F\widetilde{F} + \cdots$$

- Small mass $\Rightarrow$ large # density: field looks classical

Properties of Axion Dark Matter

$$\mathcal{L} = \frac{1}{2}(\partial^{\mu} a)^2 - \frac{1}{2} m_a^2 a^2 + C \frac{a}{f_a} G\widetilde{G} + C' \frac{a}{f_a} F\widetilde{F} + \cdots$$

- Small mass $\Rightarrow$ large # density: field looks classical
- Axions have virial velocity $v \sim 10^{-3}$
  - Coherence length $\lambda_a \sim \frac{1}{m_a v} > 1$ m $\Rightarrow$ spatially uniform on laboratory scales
  - Coherence time $\tau_a \sim \frac{\lambda_a}{v} > 4\mu$s $\Rightarrow$ light axions coherent for longer

Properties of Axion Dark Matter

$$\mathcal{L} = \frac{1}{2}(\partial^\mu a)^2 - \frac{1}{2}m_a^2 a^2 + C\frac{a}{f_a}G\widetilde{G} + C'\frac{a}{f_a}F\widetilde{F} + \cdots$$

- Small mass $\Rightarrow$ large # density: field looks classical
- Axions have virial velocity $v \sim 10^{-3}$
  - Coherence length $\lambda_a \sim \frac{1}{m_a v} > 1$ m $\Rightarrow$ spatially uniform on laboratory scales
  - Coherence time $\tau_a \sim \frac{\lambda_a}{v} > 4\mu$s $\Rightarrow$ light axions coherent for longer
- Solving E-L equations without couplings: $a = a_0 \cos(m_a t)$ with $\rho_{\mathrm{DM}} = \frac{1}{2}m_a^2 a_0^2$

Axion-Photon Coupling

Most axion detection schemes use axion-photon coupling

$$\mathcal{L} \subset \frac{1}{4} g_{a\gamma\gamma} a F\widetilde{F} = g_{a\gamma\gamma} a\, \mathbf{E} \cdot \mathbf{B}$$

[e.g., ADMX-HF (Lamoreaux) and YMCE (Baker) at Yale]

Axion-Photon Coupling

Most axion detection schemes use axion-photon coupling

$$\mathcal{L} \subset \frac{1}{4} g_{a\gamma\gamma} a F\widetilde{F} = g_{a\gamma\gamma} a\, \mathbf{E} \cdot \mathbf{B}$$

[e.g., ADMX-HF (Lamoreaux) and YMCE (Baker) at Yale]

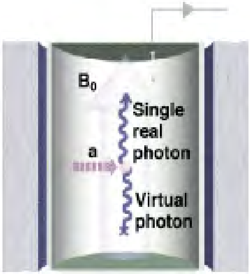

- A scattering experiment: virtual photons from **B** field as target

Axion-Photon Coupling

Most axion detection schemes use axion-photon coupling

$$\mathcal{L} \subset \frac{1}{4} g_{a\gamma\gamma} a F\widetilde{F} = g_{a\gamma\gamma} a\, \mathbf{E} \cdot \mathbf{B}$$

[e.g., ADMX-HF (Lamoreaux) and YMCE (Baker) at Yale]

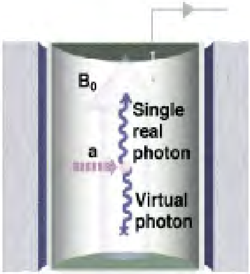

- A scattering experiment: virtual photons from **B** field as target
- Resonantly enhanced in cavity of size $L \approx \lambda_\gamma = m_a^{-1}$

Axion-Photon Coupling

Most axion detection schemes use axion-photon coupling

$$\mathcal{L} \subset \frac{1}{4} g_{a\gamma\gamma} a F \widetilde{F} = g_{a\gamma\gamma} a \, \mathbf{E} \cdot \mathbf{B}$$

[e.g., ADMX-HF (Lamoreaux) and YMCE (Baker) at Yale]

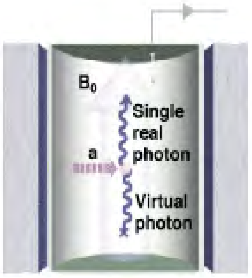

- A scattering experiment: virtual photons from **B** field as target
- Resonantly enhanced in cavity of size $L \approx \lambda_\gamma = m_a^{-1}$
- Conversion power $P \sim g_{a\gamma\gamma}^2 \Leftarrow$ unfavorable scaling, even worse without an axion source!

Axion Parameter Space

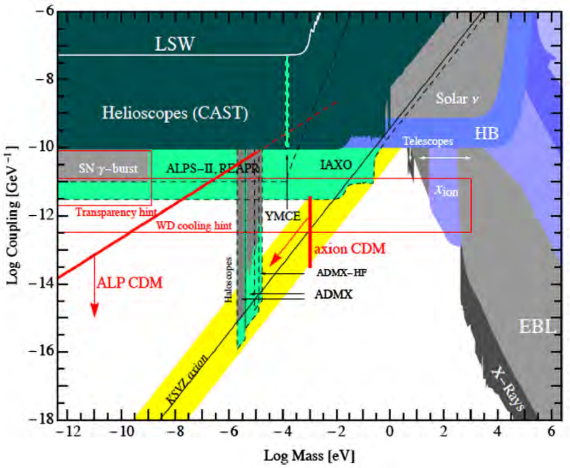

- Model band is in yellow: note $g \propto m$

Axion Parameter Space

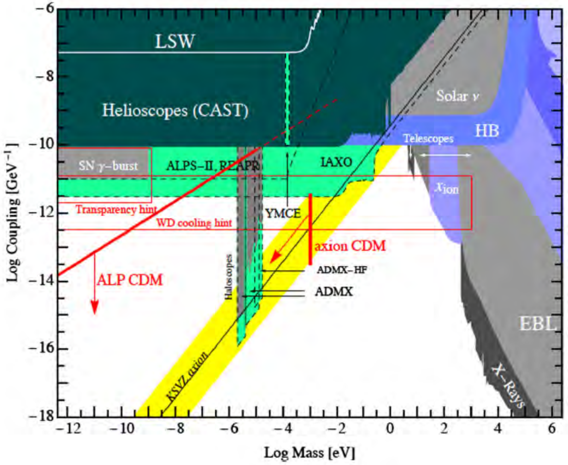

- Model band is in yellow: note $g \propto m$
- Astro bounds: $m_a \sim 1$ meV, $f_a \sim 10^9$ GeV, $\omega_a/2\pi \sim 250$ GHz

Axion Parameter Space

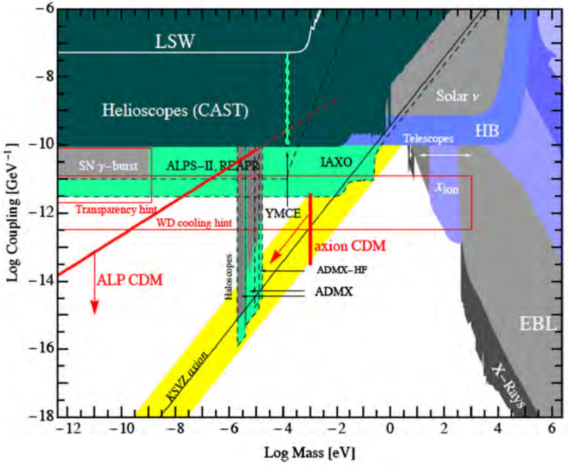

- Model band is in yellow: note $g \propto m$
- Astro bounds: $m_a \sim 1$ meV, $f_a \sim 10^9$ GeV, $\omega_a/2\pi \sim 250$ GHz
- Overclosure bound (?): $m_a \sim 1\ \mu$eV, $f_a \sim 10^{12}$ GeV, $\omega_a/2\pi \sim 250$ MHz

Axion Parameter Space

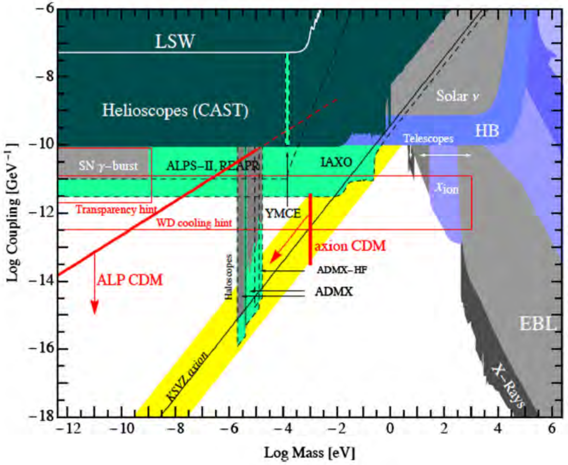

- Model band is in yellow: note $g \propto m$
- Astro bounds: $m_a \sim 1$ meV, $f_a \sim 10^9$ GeV, $\omega_a/2\pi \sim 250$ GHz
- Overclosure bound (?): $m_a \sim 1\ \mu$eV, $f_a \sim 10^{12}$ GeV, $\omega_a/2\pi \sim 250$ MHz
- GUT scale: $m_a \sim 10^{-10}$ eV, $f_a \sim 10^{16}$ GeV, $\omega_a/2\pi \sim 25$ kHz

Axion Parameter Space

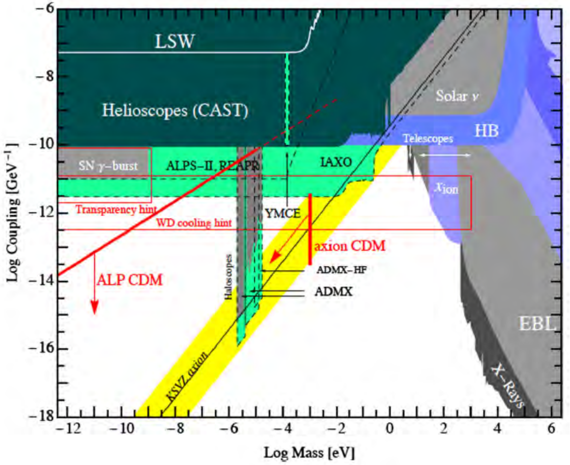

- Model band is in yellow: note $g \propto m$
- Astro bounds: $m_a \sim 1$ meV, $f_a \sim 10^9$ GeV, $\omega_a/2\pi \sim 250$ GHz
- Overclosure bound (?): $m_a \sim 1\ \mu$eV, $f_a \sim 10^{12}$ GeV, $\omega_a/2\pi \sim 250$ MHz
- GUT scale: $m_a \sim 10^{-10}$ eV, $f_a \sim 10^{16}$ GeV, $\omega_a/2\pi \sim 25$ kHz
- Planck scale: $m_a \sim 10^{-13}$ eV, $f_a \sim 10^{19}$ GeV, $\omega_a/2\pi \sim 25$ Hz

Axion Parameter Space

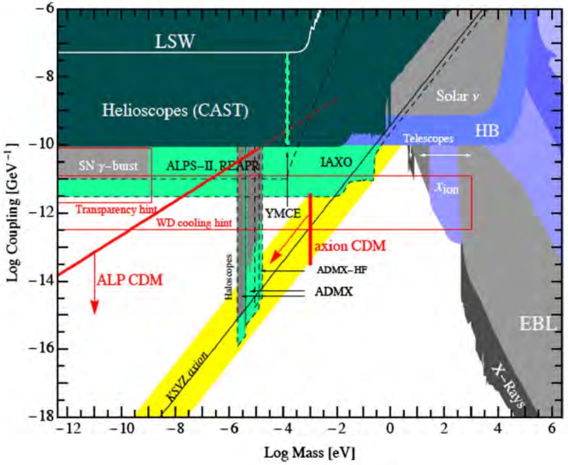

- Model band is in yellow: note $g \propto m$
- Astro bounds: $m_a \sim 1$ meV, $f_a \sim 10^9$ GeV, $\omega_a/2\pi \sim 250$ GHz
- Overclosure bound (?): $m_a \sim 1\ \mu$eV, $f_a \sim 10^{12}$ GeV, $\omega_a/2\pi \sim 250$ MHz
- GUT scale: $m_a \sim 10^{-10}$ eV, $f_a \sim 10^{16}$ GeV, $\omega_a/2\pi \sim 25$ kHz
- Planck scale: $m_a \sim 10^{-13}$ eV, $f_a \sim 10^{19}$ GeV, $\omega_a/2\pi \sim 25$ Hz
- ALPs: No relation between mass and coupling

Axion-Induced Nucleon EDMs

- A new idea: $d_n \propto \theta \Rightarrow d_n = g_d a_0 \cos(m_a t)$
  $\left(g_d = A_{\text{QCD}} f_a^{-1}\right)$

Axion-Induced Nucleon EDMs

- A new idea: $d_n \propto \theta \Rightarrow d_n = g_d a_0 \cos(m_a t)$
  $\left(g_d = A_{\mathrm{QCD}} f_a^{-1}\right)$
- If axions constitute all dark matter

$$d_n = A_{\mathrm{QCD}} \sqrt{2\rho_{DM}} \cos(m_a t) \sim 10^{-34}\, e \cdot \mathrm{cm}$$

Axion-Induced Nucleon EDMs

- A new idea: $d_n \propto \theta \Rightarrow d_n = g_d a_0 \cos(m_a t)$
  $\left(g_d = A_{\text{QCD}} f_a^{-1}\right)$
- If axions constitute all dark matter

$$d_n = A_{\text{QCD}} \sqrt{2\rho_{DM}} \cos(m_a t) \sim 10^{-34}\, e \cdot \text{cm}$$

- Parameter-free magnitude for induced AC EDM!

Axion-Induced Nucleon EDMs

- A new idea: $d_n \propto \theta \Rightarrow d_n = g_d a_0 \cos(m_a t)$
  $\left(g_d = A_{\mathrm{QCD}} f_a^{-1}\right)$
- If axions constitute all dark matter

$$d_n = A_{\mathrm{QCD}} \sqrt{2\rho_{DM}} \cos(m_a t) \sim 10^{-34}\, e \cdot \mathrm{cm}$$

- Parameter-free magnitude for induced AC EDM!
- Observable effect linear in g_d!

Static EDM Searches

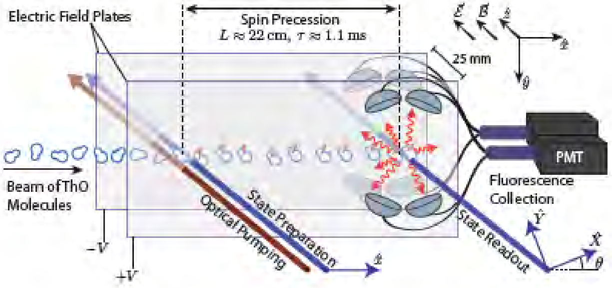

- Prepare spins $\perp$ to applied B, E fields: in time t they precess through angle $\propto \Delta U = \mu B \pm dE$

Static EDM Searches

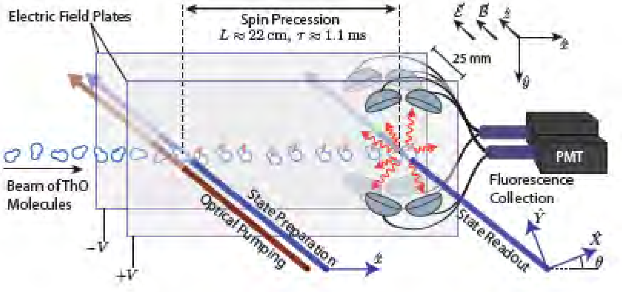

- Prepare spins $\perp$ to applied B, E fields: in time t they precess through angle $\propto \Delta U = \mu B \pm dE$
- Switch E field and subtract measurements $\Rightarrow \Delta U_d = 2dE$

Static EDM Searches

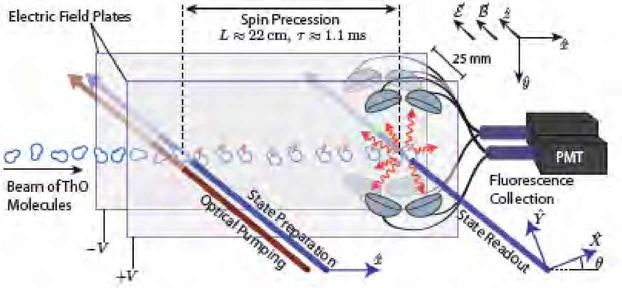

- Prepare spins $\perp$ to applied B, E fields: in time t they precess through angle $\propto \Delta U = \mu B \pm dE$
- Switch E field and subtract measurements $\Rightarrow \Delta U_d = 2dE$
- Major systematic: B field fluctuations look like additional energy splitting

Static EDM Searches

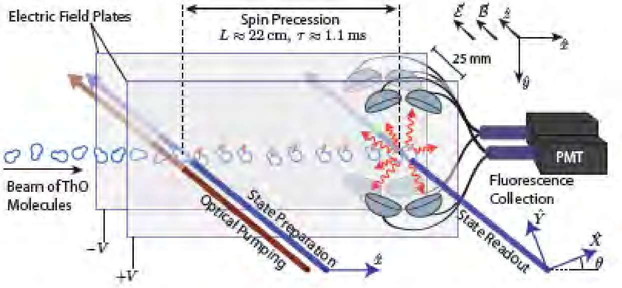

- Prepare spins $\perp$ to applied B, E fields: in time t they precess through angle $\propto \Delta U = \mu B \pm dE$
- Switch E field and subtract measurements $\Rightarrow \Delta U_d = 2dE$
- Major systematic: B field fluctuations look like additional energy splitting
- $t \sim 1$ ms $\Rightarrow$ AC EDM signal averages out.

A Measurable Effect?

- Axion-induced effect: $10^{-34}\, e \cdot \mathrm{cm}$

A Measurable Effect?

- Axion-induced effect: $10^{-34}\ e \cdot \mathrm{cm}$
- Best current limit for static neutron EDM: $10^{-26}\ e \cdot \mathrm{cm}$.

A Measurable Effect?

- Axion-induced effect: $10^{-34}\ e \cdot \mathrm{cm}$
- Best current limit for static neutron EDM: $10^{-26}\ e \cdot \mathrm{cm}$. But some reasons for hope:
  - Only need to precisely control high-frequency Fourier components of applied field

A Measurable Effect?

- Axion-induced effect: $10^{-34}\ e \cdot \mathrm{cm}$
- Best current limit for static neutron EDM: $10^{-26}\ e \cdot \mathrm{cm}$. But some reasons for hope:
  - Only need to precisely control high-frequency Fourier components of applied field
  - Resonant Detection is possible $\Rightarrow$ NMR

NMR Basics – Quantum Picture

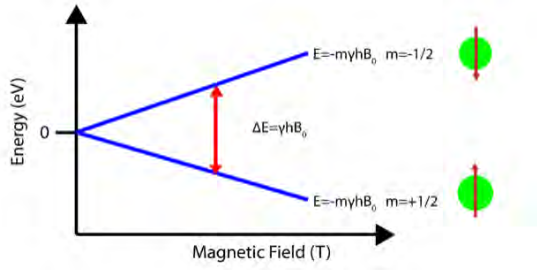

- Zeeman splittings in magnetic field $B_0\hat{z}$

NMR Basics – Quantum Picture

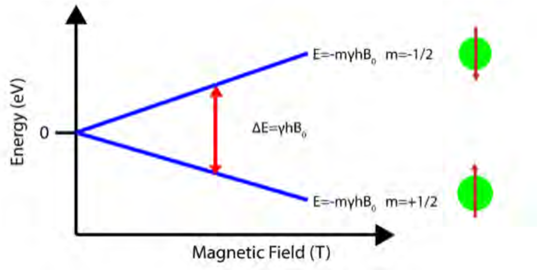

- Zeeman splittings in magnetic field $B_0\hat{z}$
  - Larmor frequency $\omega_L = \gamma B_0 \approx$ 450 MHz

NMR Basics – Quantum Picture

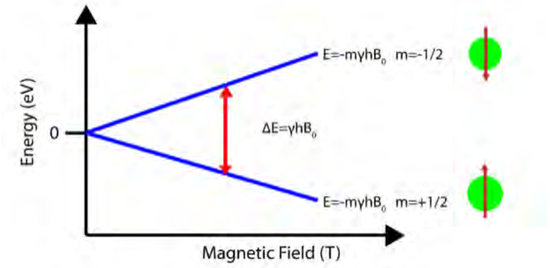

- Zeeman splittings in magnetic field $B_0\hat{z}$
  - Larmor frequency $\omega_L = \gamma B_0 \approx 450$ MHz
  - At 4 K, for ^{207}Pb in 10 T field: $N_{+1/2}/N_{-1/2} = 1 + 5 \times 10^{-3}$

NMR Basics – Quantum Picture

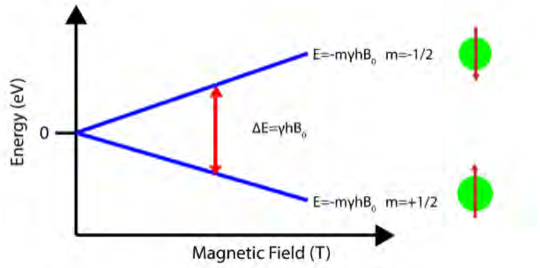

- Zeeman splittings in magnetic field $B_0\hat{z}$
  - Larmor frequency $\omega_L = \gamma B_0 \approx 450$ MHz
  - At 4 K, for ^{207}Pb in 10 T field: $N_{+1/2}/N_{-1/2} = 1 + 5 \times 10^{-3}$
- AC Transverse field at Larmor Frequency: $H_1 = \gamma B_\perp \cos(\omega_L t)$ stimulates transitions

NMR Basics – Classical Picture

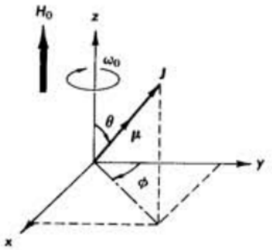

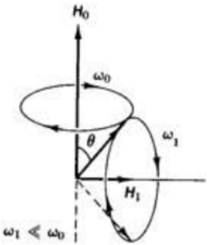

NMR Basics – Classical Picture

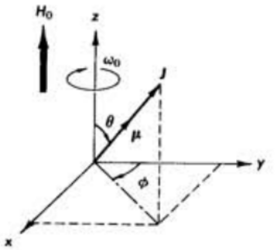

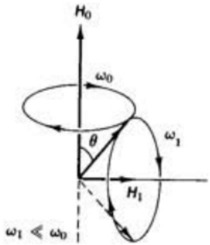

- In classical picture, spins initially precess around B_0 at Larmor frequency

NMR Basics – Classical Picture

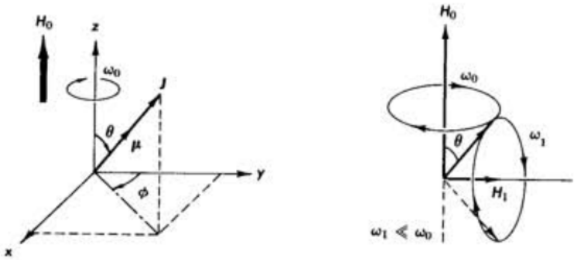

- In classical picture, spins initially precess around B_0 at Larmor frequency
- When $B_\perp$ applied at Larmor frequency, they precess around $B_\perp$ instead.

Pulsed NMR

- In most experiments, $B_\perp$ is strong, and pulsed to rotate spins into x-y plane $\Rightarrow$ "$\pi/2$ pulse"
- Use coil to detect transverse magnetization over time T_2.

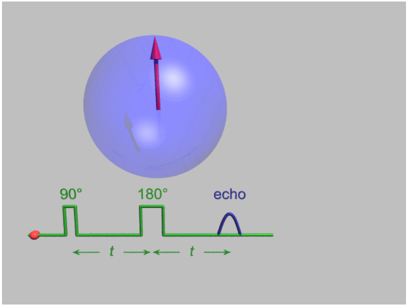

Two Timescales

- T_2: Transverse Relaxation Time

Two Timescales

- T_2: Transverse Relaxation Time
  - Due to microscopic field inhomogeneity

Two Timescales

- T_2: Transverse Relaxation Time
  - Due to microscopic field inhomogeneity
  - Resonant response has a finite width $\sim T_2^{-1}$

Two Timescales

- T_2: Transverse Relaxation Time
  - Due to microscopic field inhomogeneity
  - Resonant response has a finite width $\sim T_2^{-1}$
  - $\sim$1 ms, longer is better. Dynamic decoupling [Barrett] can yield $\sim \mathcal{O}(s)$

Two Timescales

- T_2: Transverse Relaxation Time
  - Due to microscopic field inhomogeneity
  - Resonant response has a finite width $\sim T_2^{-1}$
  - $\sim$1 ms, longer is better. Dynamic decoupling [Barrett] can yield $\sim \mathcal{O}(s)$
- T_1: Longitudinal Relaxation Time

Two Timescales

- T_2: Transverse Relaxation Time
  - Due to microscopic field inhomogeneity
  - Resonant response has a finite width $\sim T_2^{-1}$
  - $\sim$1 ms, longer is better. Dynamic decoupling [Barrett] can yield $\sim \mathcal{O}(s)$
- T_1: Longitudinal Relaxation Time
  - Induced transitions equalize population of spins in each sublevel $\Rightarrow$ Saturation

Two Timescales

- T_2: Transverse Relaxation Time
  - Due to microscopic field inhomogeneity
  - Resonant response has a finite width $\sim T_2^{-1}$
  - $\sim$1 ms, longer is better. Dynamic decoupling [Barrett] can yield $\sim \mathcal{O}(s)$
- T_1: Longitudinal Relaxation Time
  - Induced transitions equalize population of spins in each sublevel $\Rightarrow$ Saturation
  - T_1: time for populations to re-equilibrate

Two Timescales

- T_2: Transverse Relaxation Time
  - Due to microscopic field inhomogeneity
  - Resonant response has a finite width $\sim T_2^{-1}$
  - $\sim$1 ms, longer is better. Dynamic decoupling [Barrett] can yield $\sim \mathcal{O}(s)$
- T_1: Longitudinal Relaxation Time
  - Induced transitions equalize population of spins in each sublevel $\Rightarrow$ Saturation
  - T_1: time for populations to re-equilibrate
  - Due to coupling to environment

Two Timescales

- T_2: Transverse Relaxation Time
  - Due to microscopic field inhomogeneity
  - Resonant response has a finite width $\sim T_2^{-1}$
  - $\sim$1 ms, longer is better. Dynamic decoupling [Barrett] can yield $\sim \mathcal{O}(s)$
- T_1: Longitudinal Relaxation Time
  - Induced transitions equalize population of spins in each sublevel $\Rightarrow$ Saturation
  - T_1: time for populations to re-equilibrate
  - Due to coupling to environment
  - Hours at $T \sim 4$ K: shorter is better *for pulsed NMR*

NMR for an Oscillating EDM Search

- $H_1 = d_n E_\perp$ plays role of $H_1 = \gamma B_\perp$

NMR for an Oscillating EDM Search

- $H_1 = d_n E_\perp$ plays role of $H_1 = \gamma B_\perp$
- $H_1 \sim \cos(m_a t)$: frequency set by fundamental physics!

NMR for an Oscillating EDM Search

- $H_1 = d_n E_\perp$ plays role of $H_1 = \gamma B_\perp$
- $H_1 \sim \cos(m_a t)$: frequency set by fundamental physics!
- Can tune Larmor frequency by changing B_0 to get resonance

NMR for an Oscillating EDM Search

- $H_1 = d_n E_\perp$ plays role of $H_1 = \gamma B_\perp$
- $H_1 \sim \cos(m_a t)$: frequency set by fundamental physics!
- Can tune Larmor frequency by changing B_0 to get resonance
- Even with large E, H_1 is perturbative: transverse magnetization builds up continuously, limited by $\min(T_2, \tau_a)$

NMR for an Oscillating EDM Search

- $H_1 = d_n E_\perp$ plays role of $H_1 = \gamma B_\perp$
- $H_1 \sim \cos(m_a t)$: frequency set by fundamental physics!
- Can tune Larmor frequency by changing B_0 to get resonance
- Even with large E, H_1 is perturbative: transverse magnetization builds up continuously, limited by $\min(T_2, \tau_a)$
- Perturbative $H_1 \Rightarrow$ no saturation even for long T_1, so longer T_1 is better: allows use of higher-than-thermal polarizations!

CASPEr: Experimental Setup

- Apply B_0 and $E_\perp$ fields to a non-paramagnetic insulator.
- Measure transverse magnetization with sensitive magnetometer (SQUID or SERF).
- Incrementally adjust B_0 to scan axion mass range.

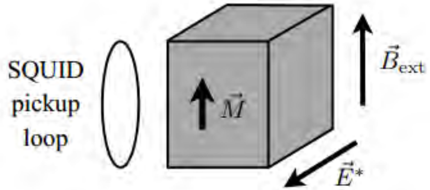

The CASPEr Signal

$$M_x(t) = np\gamma H_1 \frac{\sin\left[(\omega_L - m_a)\, t\right]}{(\omega_L - m_a)} \sin(\omega_L t)\, e^{-t/T_2}$$

$$\to np\gamma H_1\, t \sin(\omega_L t)\, e^{-t/T_2} \text{ for } \omega_L \to m_a,\ T_2 < \tau_a$$

The CASPEr Signal

$$M_x(t) = np\gamma H_1 \frac{\sin\left[\left(\omega_L - m_a\right)t\right]}{\left(\omega_L - m_a\right)} \sin\left(\omega_L t\right) e^{-t/T_2}$$
$$\to np\gamma H_1\, t \sin\left(\omega_L t\right) e^{-t/T_2} \text{ for } \omega_L \to m_a,\ T_2 < \tau_a$$

- e^{-t/T_2} due to transverse relaxation

The CASPEr Signal

$$M_x(t) = np\gamma H_1 \frac{\sin\left[(\omega_L - m_a)\,t\right]}{(\omega_L - m_a)} \sin(\omega_L t)\, e^{-t/T_2}$$
$$\to np\gamma H_1\, t \sin(\omega_L t)\, e^{-t/T_2} \text{ for } \omega_L \to m_a,\ T_2 < \tau_a$$

- e^{-t/T_2} due to transverse relaxation
- $\sin(\omega_L t)$ due to rotation of signal in *xy* plane

The CASPEr Signal

$$M_x(t) = np\gamma H_1 \frac{\sin\left[(\omega_L - m_a)\, t\right]}{(\omega_L - m_a)} \sin\left(\omega_L t\right) e^{-t/T_2}$$
$$\to np\gamma H_1\, t \sin\left(\omega_L t\right) e^{-t/T_2} \text{ for } \omega_L \to m_a,\ T_2 < \tau_a$$

- e^{-t/T_2} due to transverse relaxation
- $\sin\left(\omega_L t\right)$ due to rotation of signal in *xy* plane
- $H_1 \frac{\sin[(\omega_L - m_a)t]}{(\omega_L - m_a)}$ like a matrix element in perturbation theory: sinc function $\to \delta$ function as $t \to \infty$

The CASPEr Signal

$$M_x(t) = np\gamma H_1 \frac{\sin\left[(\omega_L - m_a)\, t\right]}{(\omega_L - m_a)} \sin(\omega_L t)\, e^{-t/T_2}$$
$$\to np\gamma H_1\, t \sin(\omega_L t)\, e^{-t/T_2} \text{ for } \omega_L \to m_a,\ \ T_2 < \tau_a$$

- e^{-t/T_2} due to transverse relaxation
- $\sin(\omega_L t)$ due to rotation of signal in xy plane
- $H_1 \frac{\sin[(\omega_L - m_a)t]}{(\omega_L - m_a)}$ like a matrix element in perturbation theory: sinc function $\to \delta$ function as $t \to \infty$
- $np\gamma$: Initial magnetization along $\hat{z}$

CASPEr: Relevant Parameters I

$$M_x(t) = np\gamma H_1 t \sin(\omega_L t)\, e^{-t/T_2} \text{ for } \omega_L \to m_a,\ T_2 < \tau_a$$

CASPEr: Relevant Parameters I

$$M_x(t) = np\gamma H_1 t \sin(\omega_L t)\, e^{-t/T_2} \text{ for } \omega_L \to m_a,\ T_2 < \tau_a$$

- $H_1 = d_n E^* \epsilon_s$

CASPEr: Relevant Parameters I

$$M_x(t) = np\gamma H_1 t \sin(\omega_L t)\, e^{-t/T_2} \text{ for } \omega_L \to m_a, \;\; T_2 < \tau_a$$

- $H_1 = d_n E^* \epsilon_s$
  - Internal fields much stronger than those available in lab: e.g. $E^* \approx 3 \times 10^8$ V/cm for ferroelectric $PbTiO_3$

CASPEr: Relevant Parameters I

$$M_x(t) = np\gamma H_1 t \sin(\omega_L t)\, e^{-t/T_2} \text{ for } \omega_L \to m_a,\ T_2 < \tau_a$$

- $H_1 = d_n E^* \epsilon_s$
  - Internal fields much stronger than those available in lab: e.g. $E^* \approx 3 \times 10^8$ V/cm for ferroelectric $PbTiO_3$
  - ϵ_s: Schiff factor: dipole interaction shielded by charges in atom. $\epsilon_s \propto Z^3 \Rightarrow$ for high-Z nucleus like Pb, $\epsilon_s \approx 10^{-2}$

CASPEr: Relevant Parameters I

$$M_x(t) = np\gamma H_1 t \sin(\omega_L t)\, e^{-t/T_2} \text{ for } \omega_L \to m_a,\ T_2 < \tau_a$$

- $H_1 = d_n E^* \epsilon_s$
  - Internal fields much stronger than those available in lab: e.g. $E^* \approx 3 \times 10^8$ V/cm for ferroelectric $PbTiO_3$
  - ϵ_s: Schiff factor: dipole interaction shielded by charges in atom. $\epsilon_s \propto Z^3 \Rightarrow$ for high-Z nucleus like Pb, $\epsilon_s \approx 10^{-2}$
- n = spin # density $\sim 10^{22}$ cm^{-3}; $\gamma \approx 0.6\mu_N$ for Pb.

CASPEr: Relevant Parameters I

$$M_x(t) = np\gamma H_1 t \sin(\omega_L t)\, e^{-t/T_2} \text{ for } \omega_L \to m_a,\ \ T_2 < \tau_a$$

- $H_1 = d_n E^* \epsilon_s$
  - Internal fields much stronger than those available in lab: e.g. $E^* \approx 3 \times 10^8$ V/cm for ferroelectric $PbTiO_3$
  - ϵ_s: Schiff factor: dipole interaction shielded by charges in atom. $\epsilon_s \propto Z^3 \Rightarrow$ for high-Z nucleus like Pb, $\epsilon_s \approx 10^{-2}$
- n = spin # density $\sim 10^{22}$ cm^{-3}; $\gamma \approx 0.6\mu_N$ for Pb.
- p: polarization fraction: can be increased from $\sim 10^{-3}$ to $\mathcal{O}(1)$ by optical pumping since T_1 is long

CASPEr: Relevant Parameters II

$$M_x(t) = np\gamma H_1 t \sin(\omega_L t)\, e^{-t/T_2} \text{ for } \omega_L \to m_a,\ T_2 < \tau_a$$

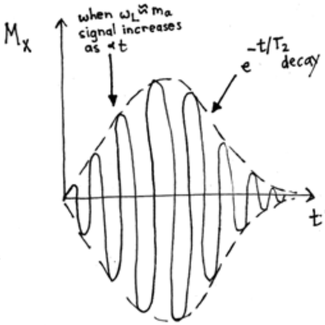

- Recall T_2: 1 ms to $\sim$ 1 s with dynamic decoupling

CASPEr: Relevant Parameters II

$$M_x(t) = np\gamma H_1 t \sin(\omega_L t)\, e^{-t/T_2} \text{ for } \omega_L \to m_a,\ T_2 < \tau_a$$

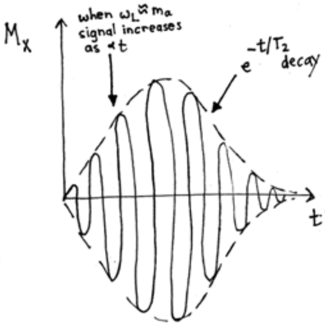

- Recall T_2: 1 ms to $\sim$ 1 s with dynamic decoupling
- τ_a : 1 ms to $\sim 10^4$ s depending on axion mass

CASPEr: Relevant Parameters II

$$M_x(t) = np\gamma H_1 t \sin(\omega_L t)\, e^{-t/T_2} \text{ for } \omega_L \to m_a,\ \ T_2 < \tau_a$$

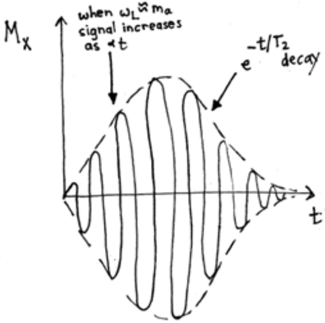

- Recall T_2: 1 ms to $\sim$ 1 s with dynamic decoupling
- τ_a : 1 ms to $\sim 10^4$ s depending on axion mass
- For now, assume $\tau_a \gg T_2$: always true without dynamic decoupling, true except for highest masses regardless

CASPEr: Relevant Parameters II

$$M_x(t) = np\gamma H_1 t \sin(\omega_L t)\, e^{-t/T_2} \text{ for } \omega_L \to m_a,\ T_2 < \tau_a$$

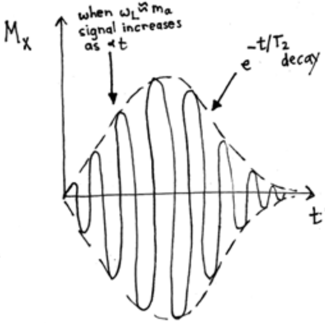

- Recall T_2: 1 ms to $\sim$ 1 s with dynamic decoupling
- τ_a : 1 ms to $\sim 10^4$ s depending on axion mass
- For now, assume $\tau_a \gg T_2$: always true without dynamic decoupling, true except for highest masses regardless

Scanning Axion Parameter Space

- Want to step γB_0 by $\sim T_2^{-1}$, take data for some time t, repeat.

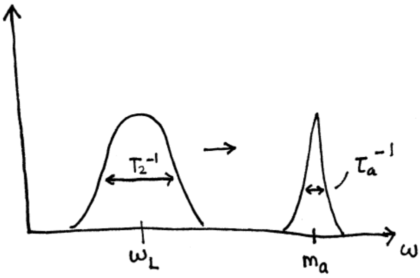

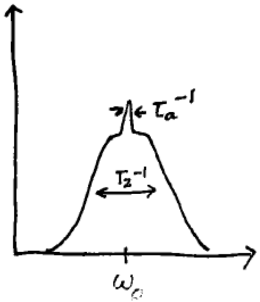

Scanning Axion Parameter Space

- Want to step γB_0 by $\sim T_2^{-1}$, take data for some time t, repeat.
- Fix a scan rate, e.g., $\mathcal{O}(1)$ range of frequencies per year: determines integration time t.

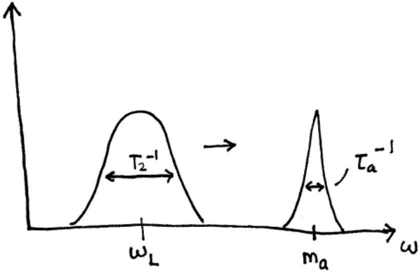

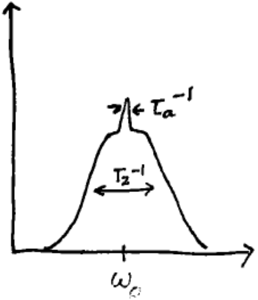

Scanning Axion Parameter Space

- Want to step γB_0 by $\sim T_2^{-1}$, take data for some time t, repeat.
- Fix a scan rate, e.g., $\mathcal{O}(1)$ range of frequencies per year: determines integration time t.
- Magnetometer noise: $\frac{10^{-16}}{\sqrt{2t}}$ T$/\sqrt{\text{Hz}}$: determines SNR $\propto t^{3/2}$

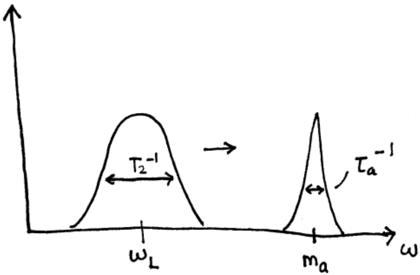

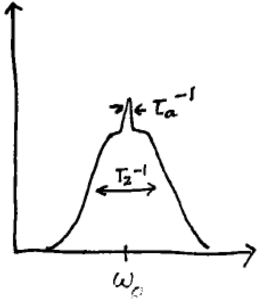

Scanning Axion Parameter Space

- Want to step γB_0 by $\sim T_2^{-1}$, take data for some time t, repeat.
- Fix a scan rate, e.g., $\mathcal{O}(1)$ range of frequencies per year: determines integration time t.
- Magnetometer noise: $\frac{10^{-16}}{\sqrt{2t}}$ T/$\sqrt{\text{Hz}}$: determines SNR $\propto t^{3/2}$
- Accessible parameter space: anywhere below 10 T $\Leftrightarrow$ 450 MHz $\sim 1\mu$eV

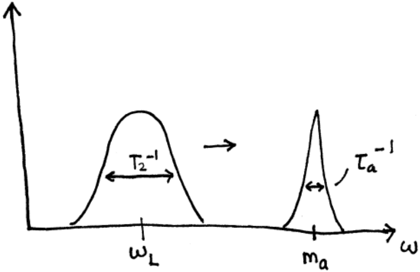

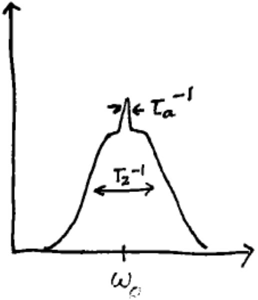

Proposed Limits

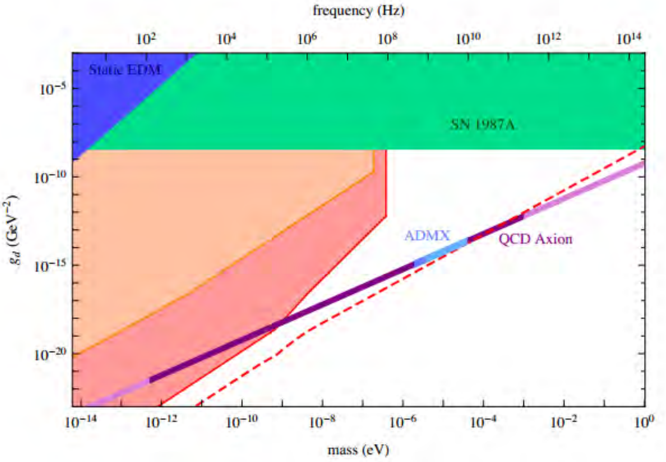

Summary

- A new idea to look for axions: look for the axion-induced EDM.
- The induced EDM is small, but could be detected using NMR techniques and sensitive magnetometers.
- Observable effect scales linearly with g_d
- Challenges
  - Precisely controlling transverse field fluctuations?
  - Lots of parameter space to cover
- Questions?

Figures from

- N. Fortson, P. Sandars, and S. Barr, Physics Today **56**(6), 33 (2003).
- A. S. Chou, U. of M. Cosmology Seminar, 2011.
- A. Melissinos, *Experiments in Modern Physics* (Academic Press, 2003).
- G. Raffelt, U. W. Axion Physics Workshop, 2012.
- G. Carosi, U. W. Axion Physics Workshop, 2012.
- A. Ringwald, Exploring the role of axions and other WISPs in the dark universe, *Physics of the Dark Universe*, 2012. Vol. 1.
- ACME Collaboration, Order of Magnitude Smaller Limit on the Electric Dipole Moment of the Electron, arXiv prepritn, 2013.
- `http://en.wikipedia.org/wiki/Nuclear_magnetic_resonance`

SNR Scaling

SNR Scaling

- For time $t < T_2$, signal increases linearly, so $SNR \propto t^{3/2}$

SNR Scaling

- For time $t < T_2$, signal increases linearly, so $SNR \propto t^{3/2}$
- For $t > T_2$, $t < \tau_a$, $M \sim dEte^{-t/T_2}$, SNR increases more slowly as signal decays

SNR Scaling

- For time $t < T_2$, signal increases linearly, so $SNR \propto t^{3/2}$
- For $t > T_2$, $t < \tau_a$, $M \sim dEte^{-t/T_2}$, SNR increases more slowly as signal decays
- For $t > \tau_a$, SNR increases by $t^{1/4}$

SNR Scaling

- For time $t < T_2$, signal increases linearly, so $SNR \propto t^{3/2}$
- For $t > T_2$, $t < \tau_a$, $M \sim dEte^{-t/T_2}$, SNR increases more slowly as signal decays
- For $t > \tau_a$, SNR increases by $t^{1/4}$
- Can understand this as incoherently adding all the bumps in quadrature